

Optical properties of small metal spheres

R. Ruppin*

Soreq Nuclear Research Centre, Yavne, Israel

(Received 8 April 1974)

The classical Mie theory for the scattering and absorption of electromagnetic radiation by a sphere is extended so as to be applicable to cases in which longitudinal polarization waves can propagate in the sphere material. The extended Mie theory is applied to the calculation of the optical properties of small metal spheres, the electronic properties of which are represented by Boltzmann-type dielectric functions. It is found that the main plasma resonance is shifted from its classical position towards the high-frequency side, and that a secondary absorption structure appears just above the plasma frequency. The dependence of these effects on the physical parameters characterizing the sphere and its surroundings is investigated.

INTRODUCTION

When calculating the optical properties of materials in which longitudinal polarization waves can propagate, the possibility of direct optical excitation of such waves has to be taken into account. A macroscopic theory, which incorporates longitudinal polarization waves, and which yields generalized boundary conditions to be employed in calculations of optical properties, has been developed by Melnyk and Harrison.¹ They have predicted the appearance of a new absorptance structure, due to the resonant excitation of bulk plasmons, in the spectra of very thin metal foils. Subsequently, measurements on silver² and potassium³ films have been performed, in which the predicted structure has indeed been observed.

Resonant excitation of bulk plasmons is also expected to occur in optical experiments performed on small metal spheres. In the classical Mie theory for the absorption and scattering properties of a sphere it is assumed that only transverse modes of the sphere are excited.^{4,5} A brief outline of the extension of the Mie theory, which allows for the excitation of longitudinal polarization waves, has recently been presented.⁶ In Sec. II a more detailed account of the extended Mie theory is given. In Sec. III this theory is applied to the calculation of the optical properties of small sodium spheres. A discussion of previous experimental and theoretical work on small metal particles and its relation to the present calculation is presented in Sec. IV.

II. EXTENDED MIE THEORY

In this section we develop a generalization of the Mie theory, which applies to the case in which the sphere material can support propagating plasma waves (i. e., plasma modes with a nonzero group velocity). We assume the material to be isotropic. The longitudinal plasma waves obey

a dispersion law of the form

$$\epsilon_L(k_l, \omega) = 0, \quad (1)$$

where ϵ_L is the longitudinal dielectric function, which depends on the frequency ω and on the magnitude k_l of the wave vector. The equation describing the propagation of transverse electromagnetic waves in the sphere material is

$$k_T^2 = \epsilon_T(k_T, \omega) \omega^2 / c^2, \quad (2)$$

where ϵ_T is the transverse dielectric function, which again depends on the frequency and on the wavevector magnitude. We wish to calculate the scattering and the absorption by a sphere of radius R , where the sphere material is characterized by given dielectric functions ϵ_T and ϵ_L .

We introduce the spherical vector-wave function,^{7,8} in terms of which all the fields will be expanded. There exist two types of transverse functions

$$\vec{M}_{\sigma mn}(\vec{r}) = \text{curl}[\vec{r} y_{\sigma mn}(\theta, \phi) z_n(kr)], \quad (3)$$

$$\vec{N}_{\sigma mn}(\vec{r}) = (1/k) \text{curl} \vec{M}_{\sigma mn}(\vec{r}), \quad (4)$$

and one type of longitudinal function

$$\vec{L}_{\sigma mn}(\vec{r}) = \text{grad}[y_{\sigma mn}(\theta, \phi) z_n(kr)]. \quad (5)$$

Here the subscript σ stands for *e* (even) or *o* (odd), according to whether $\cos m\phi$ or $\sin m\phi$ is used when multiplying by the associated Legendre polynomials $P_n^m(\cos\theta)$ in order to obtain $y_{mn}(\theta, \phi)$. $z_n(kr)$, which represents spherical Bessel or Hankel functions, is chosen as follows: $j_n(k_T r)$ for transverse electromagnetic waves inside the sphere, with k_T given by Eq. (2); $j_n(k_l r)$ for longitudinal plasma modes inside the sphere, with k_l given by Eq. (1); $j_n(k_0 r)$ for the incident wave and $h_n(k_0 r)$ for the scattered wave, both of which are defined outside the sphere. In this outer region the propagation constant k_0 is given by $k_0 = (\epsilon_M)^{1/2} \omega/c$, where ϵ_M is the dielectric constant of the

medium surrounding the sphere. In all the examples treated in Sec. III, ϵ_M is assumed to be a constant. However, the general formulas derived in this section apply also to the case of a frequency-dependent ϵ_M .

The expansion of the electric and the magnetic fields of the incident plane wave is given by⁷

$$\vec{E}_i = \vec{a}_x E_0 e^{ik_0 z - i\omega t} = E_0 e^{-i\omega t} \sum_{n=1}^{\infty} i^n \frac{2n+1}{n(n+1)} (\vec{M}_{o1n} - i\vec{N}_{e1n}), \quad (6)$$

$$\vec{H}_i = \vec{a}_y (\epsilon_M)^{1/2} E_0 e^{ik_0 z - i\omega t} = -(\epsilon_M)^{1/2} E_0 e^{-i\omega t} \times \sum_{n=1}^{\infty} i^n \frac{2n+1}{n(n+1)} (\vec{M}_{e1n} + i\vec{N}_{o1n}), \quad (7)$$

where \vec{a}_x and \vec{a}_y are unit vectors in the x and y directions, respectively.

The fields of the scattered wave are expanded in the form

$$\vec{E}_r = E_0 e^{-i\omega t} \sum_{n=1}^{\infty} i^n \frac{2n+1}{n(n+1)} (a_n^r \vec{M}_{o1n} - i b_n^r \vec{N}_{e1n}), \quad (8)$$

$$\vec{H}_r = -(\epsilon_M)^{1/2} E_0 e^{-i\omega t} \sum_{n=1}^{\infty} i^n \frac{2n+1}{n(n+1)} (b_n^r \vec{M}_{e1n} + i a_n^r \vec{N}_{o1n}). \quad (9)$$

The fields associated with the transverse electromagnetic wave inside the sphere are expanded in the form

$$\vec{E}_t = E_0 e^{-i\omega t} \sum_{n=1}^{\infty} i^n \frac{2n+1}{n(n+1)} (a_n^t \vec{M}_{o1n} - i b_n^t \vec{N}_{e1n}), \quad (10)$$

$$\vec{H}_t = -(\epsilon_T)^{1/2} E_0 e^{-i\omega t} \sum_{n=1}^{\infty} i^n \frac{2n+1}{n(n+1)} (b_n^t \vec{M}_{e1n} + i a_n^t \vec{N}_{o1n}), \quad (11)$$

and the electric field associated with the longitudinal plasma modes is

$$\vec{E}_l = E_0 e^{-i\omega t} \sum_{n=1}^{\infty} i^n \frac{2n+1}{n(n+1)} i b_n^l \vec{L}_{e1n}. \quad (12)$$

No magnetic field is associated with the longitudinal modes.

The expansion coefficients a_n^r , b_n^r , a_n^t , b_n^t , b_n^l will be obtained from the boundary conditions at $r=R$.

The tangential components of the electric and the magnetic fields have to be continuous, i. e.,

$$\vec{a}_r \times (\vec{E}_i + \vec{E}_r) = \vec{a}_r \times (\vec{E}_t + \vec{E}_l), \quad (13)$$

$$\vec{a}_r \times (\vec{H}_i + \vec{H}_r) = \vec{a}_r \times \vec{H}_t \quad (14)$$

at $r=R$, where \vec{a}_r is a unit vector in the radial direction. Unlike the case of the classical Mie theory, an additional boundary condition is needed, because we have allowed for the excitation of a longitudinal field \vec{E}_l inside the sphere. Melnyk and Harrison¹ have shown that the appropriate boundary condition for media, in which longitudinal polarization waves can propagate, is the continuity of the normal displacement current $(1/4\pi)\partial\vec{E}/\partial t$. In our case, this implies

$$\vec{a}_r \cdot (\vec{E}_i + \vec{E}_r) = \vec{a}_r \cdot (\vec{E}_t + \vec{E}_l) \quad (15)$$

at $r=R$.

Imposing the boundary conditions (13)–(15) the following five equations for the five coefficients a_n^r , b_n^r , a_n^t , b_n^t , b_n^l are obtained:

$$a_n^t j_n(k_T R) - a_n^r h_n(k_0 R) = j_n(k_0 R), \quad (16)$$

$$a_n^t [k_T R j_n(k_T R)]' - a_n^r [k_0 R h_n(k_0 R)]' = [k_0 R j_n(k_0 R)]', \quad (17)$$

$$b_n^t \frac{1}{k_T R} [k_T R j_n(k_T R)]' - b_n^r \frac{1}{k_0 R} [k_0 R h_n(k_0 R)]' - b_n^l \frac{1}{R} j_n(k_l R) = \frac{1}{k_0 R} [k_0 R j_n(k_0 R)]', \quad (18)$$

$$b_n^t \frac{n(n+1)}{k_T R} j_n(k_T R) - b_n^r \frac{n(n+1)}{k_0 R} h_n(k_0 R) - b_n^l k_l j_n'(k_l R) = \frac{n(n+1)}{k_0 R} j_n(k_0 R), \quad (19)$$

$$b_n^t k_T j_n(k_T R) - b_n^r k_0 h_n(k_0 R) = k_0 j_n(k_0 R). \quad (20)$$

Here the primes denote differentiation with respect to the argument of the radial functions. The solution for the coefficients of the scattered wave is

$$a_n^r = -\{j_n(k_T R)[k_0 R j_n(k_0 R)]' - j_n(k_0 R)[k_T R j_n(k_T R)]'\} / \{j_n(k_T R)[k_0 R h_n(k_0 R)]' - h_n(k_0 R)[k_T R j_n(k_T R)]'\}, \quad (21)$$

$$b_n^r = -\frac{c_n j_n(k_0 R) + j_n'(k_l R) \{\epsilon_M j_n(k_0 R)[k_T R j_n(k_T R)]' - \epsilon_T j_n(k_T R)[k_0 R j_n(k_0 R)]'\}}{c_n h_n(k_0 R) + j_n'(k_l R) \{\epsilon_M h_n(k_0 R)[k_T R j_n(k_T R)]' - \epsilon_T j_n(k_T R)[k_0 R h_n(k_0 R)]'\}}, \quad (22)$$

where

$$c_n = n(n+1) [j_n(k_l R)/k_l R] j_n(k_T R) (\epsilon_T - \epsilon_M). \quad (23)$$

We note that the coefficients a_n^r are the same as the corresponding coefficients of the classical Mie theory. This reflects the fact that the excitation of the magnetic modes (the modes for which \vec{E} behaves like a vector function of type \vec{M}) is not affected by the longitudinal fields. A simultaneous excitation of the electric modes (\vec{E} proportional to \vec{N}) and the longitudinal modes does, however, occur. Thus, the coefficients b_n^r differ from the corresponding Mie coefficients

$$b_n^r(\text{Mie}) = -\frac{\epsilon_M j_n(k_0 R) [k_T R j_n(k_T R)]' - \epsilon_T j_n(k_T R) [k_0 R j_n(k_0 R)]'}{\epsilon_M h_n(k_0 R) [k_T R j_n(k_T R)]' - \epsilon_T j_n(k_T R) [k_0 R h_n(k_0 R)]'} \quad (24)$$

The generalized coefficients b_n^r reduce to the Mie coefficients when $c_n = 0$. This happens when no longitudinal polarization waves can propagate in the sphere material, in which case the imaginary part of k_i becomes infinitely large.

The optical properties of the sphere are expressed in terms of the scattering, absorption, and extinction cross sections. These three cross sections are related by

$$\sigma_e = \sigma_s + \sigma_a$$

The cross sections are obtained by integrating the Poynting vector over a large concentric spherical surface in the usual way.⁷ The resulting scattering and extinction cross sections, in units of the geometric cross section πR^2 , are

$$\sigma_s = \frac{2}{(k_0 R)^2} \sum_{n=1}^{\infty} (2n+1) (|\alpha_n^r|^2 + |b_n^r|^2), \quad (26)$$

$$\sigma_e = -\frac{2}{(k_0 R)^2} \sum_{n=1}^{\infty} (2n+1) \text{Re}(a_n^r + b_n^r), \quad (27)$$

where Re denotes the real part.

III. OPTICAL PROPERTIES OF SMALL METAL SPHERES

We now calculate the optical properties of a small metal sphere using the theory of Sec. II. For the dielectric functions we will use the expressions derived by Lindhard⁹ for a degenerate electron gas in a uniform positive background

$$\epsilon_T(k, \omega) = 1 - \frac{\omega_p^2}{\omega(\omega + i/\tau)} \frac{3}{2a^2} \left(\frac{1+a^2}{a} \tan^{-1} a - 1 \right), \quad (28)$$

$$\epsilon_L(k, \omega) = 1 - \frac{\omega_p^2}{\omega(\omega + i/\tau)} \frac{3}{a^2} \left(1 - \frac{\tan^{-1} a}{a} \right) \times \left[1 + \frac{i}{\omega\tau} \left(1 - \frac{\tan^{-1} a}{a} \right) \right]^{-1}, \quad (29)$$

where

$$a^2 = -k^2 v_F^2 / (\omega + i/\tau)^2 \quad (30)$$

ω_p is the plasma frequency, v_F is the Fermi velocity, and τ is the relaxation time. We will perform calculations for sodium spheres, using the values $\omega_p = 8.65 \times 10^{15} \text{ sec}^{-1}$ and $v_F = 1.07 \times 10^8 \text{ cm/sec}$.^{1,10} For the damping factor $\gamma = 1/\omega_p \tau$ a wave-number-independent value of the order of 10^{-3} – 10^{-2} has usually been employed in related calculations of optical properties.^{1,11,12} It is, however, predicted theoretically^{13,14} and also established experimentally^{13,15} that the plasmon damping increases with the wave number k_i . This reflects the increasing possibility for plasmon decay into

electron hole pairs with increasing momentum. We will therefore use for γ the expression

$$\gamma = \gamma_0 + \alpha (k_i/k_F)^2, \quad (31)$$

where k_F is the Fermi wave number and $\gamma_0 = 0.01$, $\alpha = 0.05$. The dependence of the calculated spectra on the values of γ_0 and α will be discussed in the sequel.

The computed extinction cross section of a sodium sphere of radius 15 \AA is shown in Fig. 1. It can be seen that, unlike the classical Mie theory, our calculation predicts the appearance of a series of absorption peaks just above the plasma frequency. These peaks are due to the excitation of bulk plasmons. In our example only the first term, $n=1$, of Eq. (27) contributes to the optical properties, since the sphere size is much smaller than the wavelength of the incident beam. Another effect predicted by the calculation is the shift of the main absorption peak from its classical frequency of $\omega_p/\sqrt{3}$ towards the high-frequency side. This peak is due to the resonant excitation of a transverse electromagnetic mode of the sphere. Since the dispersion curve $\omega(k_i)$ of the plasmons starts from ω_p at $k_i=0$ and goes to higher frequencies as k_i increases, there exist no plasma modes with frequencies in the region below ω_p . In this frequency region the longitudinal polarization fields penetrate the sphere as evanescent waves

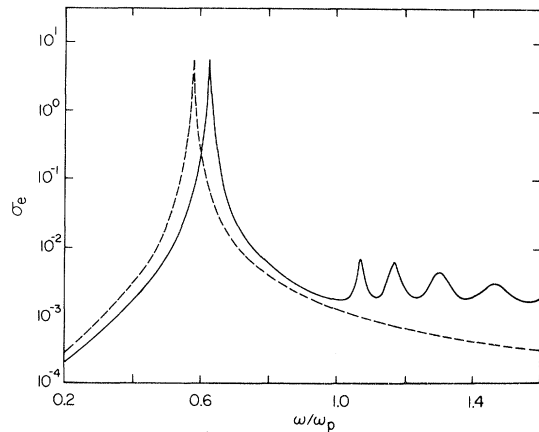


FIG. 1. Calculated extinction cross section, in units of the geometric cross section, of a sodium sphere of radius 15 \AA , with $\gamma_0 = 0.01$ and $\epsilon_M = 1$. Full curve, exact calculation; broken curve, classical Mie theory.

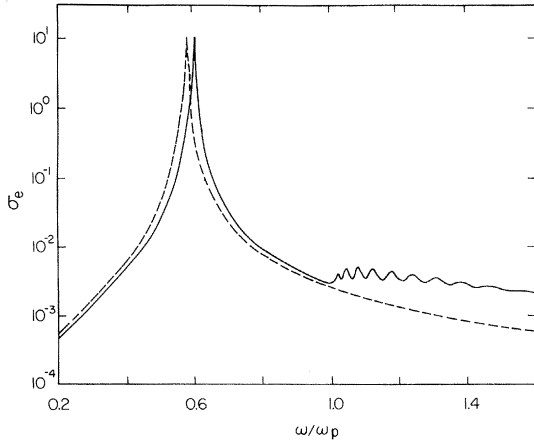


FIG. 2. Same as Fig. 1, but with the radius increased to 30 Å.

only, i.e., they have an essentially imaginary value of k_l . These evanescent fields do, however, modify the internal electric field, thus causing the shift of the main resonance from its classical position.

We next investigate the dependence of the optical properties on some of the physical parameters characterizing the sphere and its surroundings.

A. Sphere radius

The effects of increasing the radius are exemplified by Fig. 2, which shows the calculated extinction cross section of a sodium sphere of radius 30 Å. As the radius of the sphere is increased the shift of the main resonance from its classical position decreases. Physically, this follows from the fact that with increasing radius the slight evanescent penetration of the longitudinal modes into the sphere has a smaller effect on the overall field distribution inside the sphere. Another effect caused by increasing the radius is

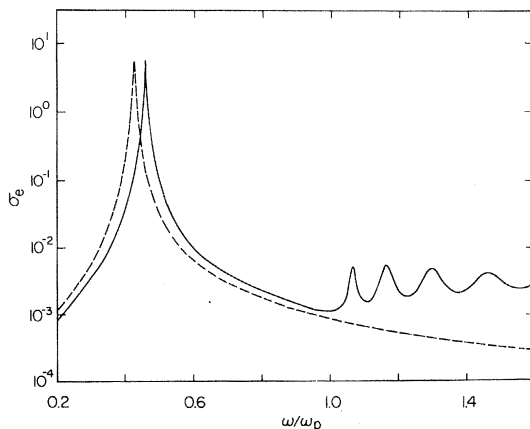


FIG. 3. Same as Fig. 1, but with $\epsilon_M = 2.25$.

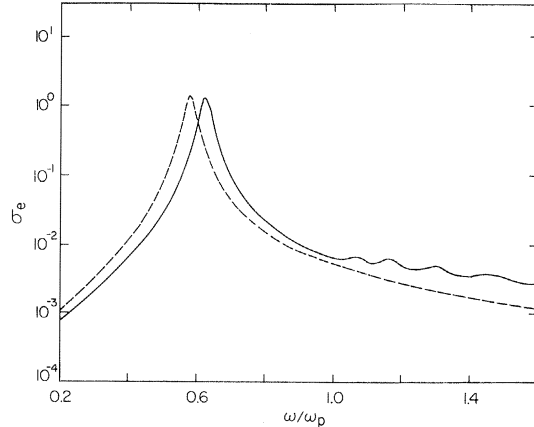


FIG. 4. Same as Fig. 1, but with $\gamma_0 = 0.04$.

the increase in the number of secondary peaks above ω_p accompanied by a decrease in their intensity. We have also performed calculations for other sphere sizes and found that for metal spheres larger than about 200 Å the calculated extinction curve deviates very little from the classical curve of the Mie theory. We note here that the strong dependence of the secondary structure above ω_p on the particle radius severely limits the experimental prospects of observing the individual peaks. Complete uniformity of size is practically unattainable in experiments performed on a collection of small metal particles. Due to the size distribution, which always exists, the absorption structure above ω_p will be smeared out, and one can only expect a broad weak absorption band to appear just above ω_p .

B. Dielectric properties of the surrounding medium

These properties enter through the dielectric constant ϵ_M , which appears in the equations of Sec. II. We have calculated the extinction cross section of a sodium sphere of radius 15 Å and with $\epsilon_M = 2.25$, which is typical for glasses which are sometimes used as an embedding medium in optical experiments on small metal particles.^{16,17} Comparing the spectrum, which is shown in Fig. 3, with that for $\epsilon_M = 1$ (Fig. 1), we find that the secondary structure above ω_p is not affected by the change in ϵ_M . The main resonance does, however, shift towards the low-frequency side with increasing ϵ_M , closely following the similar shift of the classical resonance. The latter resonance, which for $\epsilon_M = 1$ appeared at the frequency $\omega_p/\sqrt{3}$, occurs at the frequency $\omega_p/(1 + 2\epsilon_M)^{1/2}$.

C. Plasmon damping

It is naturally expected that an increase of the plasmon damping will make the absorption peaks smaller and broader. The damping parameter

γ , given by Eq. (31), can be varied either uniformly by changing the value of γ_0 , or in a wave-number-dependent way by changing the value of α . Obviously, the effect of an increase in α will become more and more pronounced as one moves away from ω_p to higher-order peaks. An increase in γ_0 will affect all the peaks in a roughly uniform way. As an example we have calculated the extinction cross section of a sodium sphere of radius 15 Å with an increased damping of $\gamma_0=0.04$ (and with $\alpha=0.05$ as before). Comparing the calculated spectrum (Fig. 4) with that corresponding to $\gamma_0=0.01$ (Fig. 1), it is found that the main resonance, as well as the subsidiary peaks above ω_p , are all broadened, as expected, but their positions remain unchanged. The dependence of the spectrum on the damping again imposes limitations on the potential experimental detection of the subsidiary structure. In very small metal spheres the mean free path of the electrons is reduced due to collisions with the surfaces.¹⁷ This implies that the damping parameter of a small sphere will be larger than that of a bulk sample. Consequently, the absorption structure above ω_p will be severely damped. In sodium spheres of radius 15 Å, assuming that the electronic mean free path is equal to the sphere diameter, one obtains $\gamma_0=0.04$, as in Fig. 4. Taking the electronic mean free path as equal to the sphere radius will double this value to $\gamma_0=0.08$ and the corresponding peaks in the spectrum above ω_p will barely be observable.

We have applied the theory to the cases of sodium and potassium⁶ spheres since these are the two most free-electron-like metals, and the use of Boltzmann-type dielectric functions seems reasonable. Recent calculations by Haque and Kliever¹⁴ have shown that the incorporation of energy-band-structure effects does, however, modify the plasmon dispersion curves or, equivalently, the longitudinal dielectric function, of sodium and potassium. One of the interesting effects found was the dependence of the plasmon dispersion on the direction of propagation. This means that ϵ_L will depend on the wave vector \vec{k} , and not only on its magnitude, as assumed in our calculation. This anisotropy will simply cause a broadening of the absorption peaks occurring above ω_p . This follows from the random distribution of the spherical crystallites in experimental situations, which leads to the excitation of bulk plasmons corresponding to various directions of propagation. For practical purposes this broadening is unimportant since the absorption structure above ω_p is smeared out anyway because of the size distribution effects described above.

IV. DISCUSSION

A related theoretical investigation of the optical properties of metallic colloids, in which the ex-

citation of longitudinal modes was taken into account, has been presented by Clanget.¹² He employed boundary conditions due to Sauter,¹⁸ which differ from those due to Melnyk and Harrison,¹ which were used in this paper. According to Sauter the normal component of the conduction current is continuous. Melnyk and Harrison¹ have argued that for time dependent fields no distinction between polarization and conduction currents should be made, and hence the normal component of their sum should be continuous. From Maxwell's equations it readily follows that the latter requirement is equivalent to the condition of continuity of the normal displacement current, which has been used in Sec. II. Clanget's calculations were the first to predict the appearance of a secondary absorption structure above ω_p in the spectrum of a small metal sphere. The dependence of this structure on the damping factor γ_0 , as given by Clanget is, however, completely different from that obtained in our calculation. Whereas we find that an increase in γ_0 only leads to the broadening of the absorption peaks, according to Clanget's calculation it also causes very substantial shifts of the absorption peaks, which seems unphysical. The behavior of the main resonance has not been discussed by Clanget. In the works of Melnyk and Harrison¹ and Clanget,¹² as well as in our preliminary calculations,⁶ a wave-number-independent plasmon damping term was used. This gave rise to the unrealistic feature that the series of secondary peaks above ω_p extended towards the high frequency side without decreasing in magnitude. Due to our use of a wave-number-dependent damping, Eq. (31), the calculated peaks become progressively more damped as one moves to higher frequencies. We have incorporated the wave-number-dependent damping term so as to compensate for the fact the dielectric functions (28) and (29) are not realistic enough. In doing so we have been guided by the results of elaborate calculations of plasmon dispersion curves including band structure effects,¹⁴ which indicate a general trend of increased damping for increasing values of the wave vector. Although the present calculations might perhaps be refined by using more sophisticated dielectric functions, we expect that this will not cause any significant modifications of the two main effects predicted here, i. e., the shift of the main resonance and the appearance of a secondary absorption structure.

As regards the possibility of experimental observation, we discuss separately each of the two effects predicted by the theory. To observe the shift of the main resonance from its classical position it is clearly advantageous to use the smallest spheres possible. The existence of a nonuniformity of sphere sizes will cause a broaden-

ing of the main peak, but this should not preclude the observation of its shift from the classical value. Deviations of the particles from spherical shape should, however, be avoided, since the main resonance frequency is strongly shape dependent. The shift of the main resonance has apparently been detected by Duthler *et al.*,¹⁹ who have observed the resonance scattering of light from sodium particles of less than 50-Å radius. They found that the main scattering maximum (which should appear at the same frequency as the extinction maximum of our calculation) was shifted from the classically predicted value of 376 nm and occurred instead between 310 and 330 nm, the exact location depending on experimental conditions. Duthler *et al.*¹⁹ have ruled out the possibility of a shape effect (i.e., deviation from spherical shape) by considering the polarization and the width of the scattered light. The observed shift of the main resonance towards the high-frequency side qualitatively agrees with our calculation, but is somewhat larger than expected. For sodium spheres of radius 15 Å, which is a typical experimental radius, the calculated maximum ap-

pears at 350 nm. To obtain a theoretical shift of the order of the observed one, a radius smaller than 10 Å has to be assumed.

The second effect, i.e., the appearance of a series of subsidiary maxima above ω_p , also becomes more prominent as the radius decreases, provided that the damping term γ is kept constant. Physically, however, the damping increases with decreasing radius due to the mean free path effect mentioned in Sec. III. For large damping the secondary structure is less pronounced and more difficult to observe. Thus, one has to compromise between the two requirements of small radius on the one hand, and small damping on the other hand. It seems that the optimal sphere radii for observation of this effect are around 30–60 Å. As already noted in Sec. III, the individual peaks will not be discernible. Because of the sphere size distribution, which can hardly be avoided, the secondary structure will be smeared out so that only one wide absorption band just above ω_p is expected. Such a band indeed appears in the scattering spectra of small sodium spheres given by Duthler *et al.*¹⁹

*Present address: Dept. of Physics, University of Essex, Colchester, England.

¹A. R. Melnyk and M. J. Harrison, *Phys. Rev. B* **2**, 835 (1970).

²I. Lindau and P. O. Nilsson, *Phys. Scripta* **3**, 87 (1971).

³M. Anderegg, B. Feuerbacher, and B. Fitton, *Phys. Rev. Lett.* **27**, 1565 (1971).

⁴G. Mie, *Ann. Phys. Leipz.* **25**, 377 (1908).

⁵M. Kerker, *The Scattering of Light and Other Electromagnetic Radiation* (Academic, New York, 1969).

⁶R. Rupp, *Phys. Rev. Lett.* **31**, 1434 (1973).

⁷J. Stratton, *Electromagnetic Theory* (McGraw-Hill, New York, 1941).

⁸P. M. Morse and H. Feshbach, *Methods of Theoretical Physics* (McGraw-Hill, New York, 1953).

⁹J. Lindhard, *Kgl. Danske Videnskab. Selskab, Mat.-Fys. Medd.* **28**, No. 8 (1954).

¹⁰J. C. Sutherland, E. T. Arakawa, and R. N. Hamm, *J. Opt. Soc. Am.* **57**, 645 (1967).

¹¹W. E. Jones, K. L. Kliewer, and R. Fuchs, *Phys. Rev.* **178**, 1201 (1969).

¹²R. Clanget, *Optik* **35**, 180 (1972).

¹³B. W. Ninham, C. J. Powell, and N. Swanson, *Phys. Rev.* **145**, 209 (1966).

¹⁴M. S. Haque and K. L. Kliewer, *Phys. Rev. B* **7**, 2416 (1973).

¹⁵P. Zacharias, *Z. Phys.* **256**, 92 (1972).

¹⁶R. H. Doremus, *J. Chem. Phys.* **40**, 2389 (1964).

¹⁷U. Kreibitz and C. V. Fragstein, *Z. Phys.* **224**, 307 (1969).

¹⁸F. Sauter, *Z. Phys.* **203**, 488 (1967).

¹⁹C. J. Duthler, S. E. Johnson, and H. P. Broida, *Phys. Rev. Lett.* **26**, 1236 (1971).